eXPRESS Polymer Letters Vol.15, No.10 (2021) 940–956
Available online at www.expresspolymlett.com
https://doi.org/10.3144/expresspolymlett.2021.76

Strain-induced consolidation of partially disentangled polypropylene

A. Pawlak[1*], *I. Vozniak*[1], *J. Krajenta*[1], *V. Beloshenko*[2], *A. Galeski*[1]

[1]Centre of Molecular and Macromolecular Studies, Polish Academy of Sciences, Sienkiewicza Street, 112, 90363 Łodz, Poland
[2]Donetsk Institute for Physics and Engineering named after A.A. Galkin, National Academy of Sciences of Ukraine, pr. Nauki 46, 03028 Kyiv, Ukraine

Received 13 April 2021; accepted in revised form 29 May 2021

Abstract. The role of entanglement of polymer chains in the merging and consolidation of polypropylene (PP) powder grains was elucidated. The entanglement density was varied by the dissolution of PP and precipitation. The differently entangled powders were sintered, without melting, applying severe plastic deformation by equal channel multiangular extrusion (ECMAE). Compaction by ECMAE resulted in healing of the interparticle pores, as well as the formation of a fibrillar structure, more significant in the case of disentangled PP. Lower entanglement density also led to the formation of thicker interfaces and to new crystals due to the strain-induced crystallization of slacks between entanglement knots. The consolidation of disentangled powder was drastically better than entangled PP powder: the yielding in compression occurred via crystallographic slips in the sintered disentangled powder while in the entangled PP powder through a series of weak elements and defects, due to much poorer compactness and cohesion. It was suggested that better consolidation of disentangled PP powder is due to reptation of longer slacks between entanglement knots and also due to sideway motions of their loops.

Keywords: *processing technologies, polypropylene, disentanglement, sintering, solid-state extrusion*

1. Introduction

The macromolecular entanglements have been the subject of research for many years. Based on rheological studies, it is assumed that polymer in melt contains a certain characteristic, equilibrium density of entanglements, depending on the type of polymer, but not on its macromolecular mass [1, 2]. The density of entanglements is best characterized by a molecular mass between entanglement knots [3]. In crystalline polymers, the entanglements are rejected during crystallization and concentrated in the amorphous phase [4].

Several methods to obtain polymers with reduced entanglement density are available. There are two main approaches. The first is the crystallization during polymerization, mostly applied for ultrahigh molecular weight polyethylene (UHMWPE) [5, 6] and poly(tetrafluoroethylene) (PTFE) [7]. The conditions of polymerization are such that the growing polymer chains are separated and can crystallize immediately [5, 8, 9]. The second group of methods is based on dissolving the polymer [10–12]. In the diluted solution, the number of contacts between macromolecules, among them entanglements, strongly depends on the concentration. The key issue is maintaining the state of reduced entangling by transforming the polymer from solution to solid-state. One option is to freeze the solution rapidly with subsequent removal of solvent [13, 14]. The second possibility, used for example, for polypropylene, is the initiation of the crystallization process, which stabilizes the structure of the rest of the polymer [15].

*Corresponding author, e-mail: apawlak@cbmm.lodz.pl

The mechanical properties of partially disentangled polymers were the subject of only limited and uncompleted studies. The first observations of different mechanical properties of polymers with reduced entanglements were from the 80s of the 20th century when Lemstra and Smith [12, 16, 17] performed experiments by spinning polymer solutions after gelation. They observed that PE or PP gels could be spun to very high draw ratios, forming very strong fibers. The large deformations resulted from the reduction of entanglements concentration in the gel [12, 18].

The disentangled UHMWPE was used for the preparation of highly oriented tapes or films, characterized by the high tensile strength [11, 12, 17] and ability to deform 200–300 times [16, 18]. The comparison of mechanical properties of differently entangled polyethylenes, tested in compression, showed that polyethylene with fewer entanglements in the amorphous phase is capable of reaching a larger plastic deformation, with a delayed strain-hardening step [19]. Similar conclusions followed from the study of the deformation of less entangled polypropylene [20]. In addition, less entangled polypropylenes are characterized by significantly lower elastic modulus. The properties of ultrahigh molecular weight polypropylene (UHMWPP) films obtained from the gel solutions were examined by Ogita *et al*. [21], Ikeda *et al*. [22], and Chen *et al*. [23]. It was possible to obtain a deformation ratio of 60 [20].

The evolution of disentangled polypropylene internal structure with tensile deformation was studied by Pawlak *et al*. [24]. The yield stress and strain values were attributed to crystal plasticity and were independent of the concentration of entanglements. However, the strain hardening phase of deformation depended on the density of the entanglements, and the observed increase of stress was faster when PP was more entangled. The disentangling of the polymer supports enhanced cavitation during tensile drawing. The cavitation in disentangled PP was possible even at a high deformation temperature of 100 °C.

Usually, the product of disentangling is a fine-grained powder. It should be carefully processed to maintain the state of disentangling. The studies of melting of many polymers have shown that short processing, even at high temperatures, is possible without the risk of serious re-entangling [24]. However, the use of high temperature should be limited if possible, which is why sintering of polymer powders in the solid state was used in our material preparation.

Conventional polymer sintering is a three-stage process [25, 26]. The first stage is powder densification through pre-compaction, which is aimed at latching the polymer grains. It is usually performed below its melting or glass transition temperature. The second stage is the heating of the densified grains close to but below its melting or glass transition temperature in order to accelerate the diffusion of chains across the interfaces of adjacent grains. This leads to the consolidation of the interfaces by chain entanglement. At this stage, two parameters play a major role, namely time and temperature. Finally, in the third stage, crystallization for semicrystalline polymers or vitrification for amorphous ones takes place. In the case of semicrystalline polymers, it is also possible to promote the strengthening of the interfaces by cocrystallization of the chains after their interdiffusion. The cocrystallization process consists of the formation of new crystallites across the interfacial regions of the adjacent powder particles.

The chain diffusion process is determined by reptation kinetics [27]. The latter strongly depends on the molecular mass of the polymer and exhibits an equivalent dependence on time t and temperature T. According to [28, 29], the re-entanglement rate in the interfacial region is proportional to $(Tt)^{\gamma}$, where the γ value can be either 1/2 or 1/4 [26]. Another factor affecting chain mobility is the type of crystal lattice (polymer crystal size) and the presence of high pressure. For instance, the use of hexagonal UHMWPE crystals possessing high chain mobility makes it possible to generate a highly cohesive material and determines the promotion of cocrystallization of chains from adjacent crystals [30, 31].

High pressure is also needed to produce a large contact surface area for intimate molecular contact at particle boundaries enabling interfacial diffusion [32]. However, there is a critical value of the pressure at which the interfacial diffusion starts to decrease. The relative rate of interdiffusion and cocrystallization processes also remains important since too high a crystallization rate can significantly hinder further chain interdiffusion and thus reduce the sintering.

As the above review shows, there is no detailed research on the effect of the degree of entanglement of polymer grains on the sintering consolidation efficiency. Besides, the sintering can be carried out in a way that results in simultaneous deformation and orientation of the polymer. No studies have been conducted so far on how such deformation occurs at

the microscale, especially if it leads to large plastic deformation. From the point of view of properties of the partially disentangled polymer, the use of sintering avoids the melting of the disentangled polymer powder. The possibility of simultaneous research on the processes of sintering and plastic deformation of entangled polymers is provided by an equal channel angular extrusion [33, 34], with the back pressure (ECAE-BP) method. ECAE-BP is now a well-known process of severe plastic deformation [35–39]. We suggest that it can be used to consolidate polypropylene disentangled powders at low temperatures (below T_g in amorphous and below T_m in semicrystalline materials) as intense shearing associated with hydrostatic pressure occurs at the intersection of the two channels with equal cross-sections. Relatively low temperatures of the sintering prevent noticeable thermal degradation. This also eliminates the need to use any additional plasticizers to form sufficient chain entanglement throughout the polymer. It is known that the use of plasticizer results in a decrease in the processing temperature, *i.e.*, allows avoiding the undesirable thermal decomposition process, but leads to a deterioration in strength characteristics of natural polymers. Polyamide 12 [39], UHMWPE [38], cotton linter microcrystalline cellulose particles [40], maple hardwood particles [41, 42], as well as natural polymers such as wheat starch and wheat gluten, have been successfully sintered by ECAE-BP. It has been shown that ECAE-BP reduces the polymer crystallinity and promotes chain penetration, intermolecular interaction, and thermal crosslinking between polymer particles.

The goal of this research is to use the severe plastic deformation concept to probe the efficiency of the modified ECAE-BP version, namely, the equal-channel multiangular extrusion (ECMAE) process for sintering polymer particles into a bulk material at lower temperatures. The peculiarity of ECMAE is that there are several zones of shear deformation in one device, as opposed to one zone of shear deformation in the case of ECAE-BP, which allows the accumulation of high plastic deformation per one cycle [43]. Although the original shape of the sample can be maintained in the ECMAE process, as it passes through a series of channel intersections, multiple plastic deformations occur, changing the internal microstructure of a polymer. Two polypropylenes in the entangled (with equilibrium density of entanglement of macromolecules) or partially disentangled states, determining different long-range chain mobility during stress events, were used to study the effect of the initial polymer morphology on the efficiency of three processes: crystallization, interdiffusion (re-entanglement) and accommodation of plastic deformation.

2. Experimental

2.1. Materials

Isotactic polypropylene Novolen 1100 N, produced by BASF, having molecular mass M_w = 250 kg/mol, density 0.936 g/cm^3, and melt flow index, MFI = 11 g/10 min was used in the experiments. Xylene (from Chempur, Poland) was used for the dissolution of PP and producing disentangled powder.

2.2. Preparation of PP nascent powders

The PP solutions were prepared by dissolution 2 wt% (dilute solution) of polymer in hot xylene at the temperature of 130–135 °C. The time of dissolution was 1 h. Then the temperature was slowly decreased at the rate of 15 °C/h. When the temperature reached approximately 80 °C, a gel begins to form inside the flask. The solution with gel was cooled further down to 40 °C, and the gel was filtered and dried. After drying, a powder with a limited density of entanglement of macromolecules was obtained. The same procedure was used to prepare the polypropylene powder from a concentrated solution with a content 10 wt% of polymer. According to theoretical considerations [13, 44], polypropylene obtained from a 10 wt% solution should nearly maintain the equilibrium density of entanglements, while the polymer obtained from the 2 wt% concentration should be partially disentangled. The entanglement density in both of these polypropylenes was the subject of research in our previous work [45]. Using the rheological method, the molecular mass between entanglement knots was found to be 12600 g/mol for polypropylene from 10 wt% solutions and 18 000 g/mol for polypropylene from 2 wt% solutions. The same but completely entangled polypropylene showed the molecular mass between entanglement knots of 9900 g/mol. The polymer obtained from a 10 wt% solution is designated as PP10%, while the disentangled polymer obtained from a 2 wt% solution as PP2%.

2.3. ECMAE sintering of PP

ECMAE sintering was carried out in three stages: obtaining a compacted sample, pre-heating the sample, extrusion of the sample. At the first stage, the

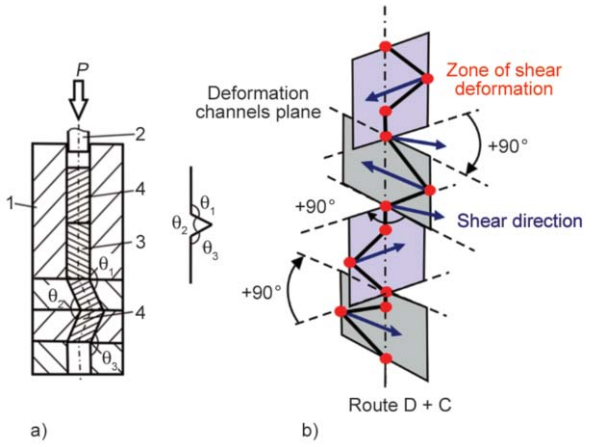

Figure 1. a) Scheme of ECMAE process: 1 – die, 2 – punch, 3 – polymeric billet, 4 – subsidiary billets. Only one segment is shown here. (Adapted from [43]) ; b) The sketch of channel arrangement in the applied D + C route.

powder was introduced into a cylindrical press mold with an internal diameter of 15 mm and a channel length of 90 mm and compacted with a rod (3 fillings with pre-pressing); the resulting billet 55 mm long was pressed out of the mold. At the second stage, the sample was heated in an oven to $T = 130\,°C$ for 15 minutes, *i.e.*, below the melting temperature (~165 °C). At the third stage, ECMAE was carried out by pressing the hot sample through a device consisting of several pairs of channels of the same diameter intersecting at varied angles θ_i: $\theta_1 = 135°$, $\theta_2 = 90°$, $\theta_3 = 135°$ (Figure 1). The inlet and outlet channels were made vertically coaxial to keep the billet pointing in the right direction. A detailed description of ECMAE is presented in Beloshenko *et al.* [46]. ECMAE parameters were: the deformation intensity $\Delta\Gamma = 0.83$, the accumulated strain $e = 8.5$. The deformation route was D + C, as in Figure 1, with the extrusion temperature of 130 °C and the extrusion rate of 0.6 mm/s. The maximum pressure during ECMAE was 360 MPa.

The primary benefit of route D + C is that the plastic deformation is accumulated inside the polymeric billet while its shape is restored due to the sign-alternating character of the spatial arrangement of the shear vectors in mutually perpendicular deformation channels planes.

2.4. Characterization

Thermal analysis of PP samples was conducted using the differential scanning calorimeter (DSC) TA Instruments Q20 (Thermal Analysis, USA). The melting thermograms were recorded during heating from 20 to 185 °C, with the rate of 10 °C/min, under nitrogen flow. The weight crystallinity X_c, was estimated on the basis of the heat of melting of the sample using Equation (1):

$$X_c = \frac{\Delta h_f}{\Delta h_{f100}} \cdot 100\% \tag{1}$$

where Δh_f is the heat of melting of the sample determined from the DSC melting curve and $\Delta h_{f100} = 209$ J/g [47] is the heat of melting of 100% crystalline PP.

The density of extruded material was determined using a pycnometer filled with ethanol, according to PN-EN ISO-1183-1 standard. The sample mass was at least 1 g. The measurements were repeated at least three times.

The morphologies were examined using the scanning electron microscope Jeol JSM 6010LA (SEM) with high vacuum mode and accelerating voltage of 15 kV. Cryogenic fracture and selective etching after microtoming were applied to reveal the inner structure of PP. For the cryogenic fracture, the samples were placed in liquid nitrogen for 15 minutes; finally, the samples were cryogenically fractured along the extrusion direction. Some samples for microscopic studies were prepared by etching. Before etching, the samples were cut with a microtome (Tesla) equipped with a glass knife in order to expose a flat and smooth cross-section surface. PP samples were permanganate etched according to the procedure developed originally by Olley *et al.* [48]. Typically, samples were etched for 1 hour at room temperature in the mixture containing 1 wt% of $KMnO_4$ dissolved in a 1:1 vol./vol. mixture of concentrated sulfuric and phosphoric acid. Details of the procedure are given in [49]. Afterward, exposed surfaces of samples were coated with a fine gold layer (about 10 nm thick) by ion sputtering.

Three X-ray methods were used for the determination of the structure before and after ECMAE process. Wide-angle X-ray scattering (WAXS) camera was used for the determination of lamellar orientation. 2-D WAXS images were registered with a flat X-ray camera equipped with imaging plates (Fuji) and coupled to Cu K_α source (sealed tube operating at 30 kV and 50 mA, Philips). Exposed imaging plates were analyzed with a Vista Scan View system (Durr Dental). In addition, the X-ray measurements were performed with a diffractometer. X-ray diffractometer in the transmission mode, equipped with a Philips

generator and an X-ray tube of Cu K_α line radiation, was used for this purpose. The radiation was registered as a function of the 2θ angle by a scintillation counter; the measurement step was 0.05°.

Small-angle X-ray scattering (SAXS) was used for the determination of structural changes during deformation, among them for the determination of a long period. A 1.2 m long Kiessig-type SAXS camera was coupled to GeniX Xenocs X-ray system (Cu K_α, wavelength 0.154 nm, operating at 50 kV and 1 mA). The scattered radiation was recorded by Pilatus 100K detector. The SAXS system allowed for the resolution of scattering objects up to 60 nm in size.

The mechanical properties of polypropylenes were tested during uniaxial compression using the Instron 5582 tensile testing machine. The temperature of the test was 25 °C. The sample was compressed at a rate of 5% of the initial thickness per minute. The samples were cylindrical in shape with 12 mm diameter and 5 mm thickness. From materials processed by the ECMAE method, they were cut in two directions: perpendicular to the direction of extrusion and parallel to this direction. The number of samples tested was limited to three by material availability, but the analysis of the force-displacement curves showed good repeatability of results.

Microhardness, H, was determined using a microhardness tester. The indenter was a tetrahedral diamond pyramid with a vertex angle of 136°. The pyramid was fluently pressed unto the sample at the loading of 0.5 N. The value of microhardness was estimated by the formula $H = 0.1854\ F/d^2$, where F – loading [N], d – diagonal of the indentation [mm], and $d^2/0.1854$ – area of the lateral surface of produced pyramidal indentation. For H, the relative error was not higher than 5%.

3. Results and discussion

During the processing of polymer powders by the ECMAE method, two processes occur in parallel and partly at the same time. These are grain sintering, leading to the formation of a uniform material and plastic deformation of the crystalline and amorphous components of a polymer. The conventional sintering process is often studied in terms of two processes: interdiffusion and crystallization or entangling of diffusing macromolecules. These processes determine the efficiency of consolidation and the final properties of the material. The interdiffusion process in the solid state is diffusion across particles contact points of polymer chains of the amorphous phase, as well as molten crystalline phase if melting is possible. Evidently, the deeper the chains diffuse, the more interparticle space is formed, and the particles coalesce more. An additional crystallization may happen near the grain boundary with the participation of diffusing macromolecules. On the one hand, this crystallization contributes to the strengthening of the interfaces, and on the other hand, may affect the interdiffusion process leading to its hindering.

In this regard, it makes sense to consider the possibility of implementing both of these processes in the case of ECMAE-sintering, after comparing the structures of the initial and preliminary compacted samples.

3.1. Morphologies of preliminary compacted samples

The preliminary compaction process with annealing at an extrusion temperature of 130 °C for 15 minutes, giving samples to ECMAE, should result in closer contact between the powder particles. To assess this, morphologies were analyzed using a scanning electron microscope. Figure 2 shows the morphologies of the powders after polymer compaction. It can be seen that such preliminary processing of PP samples preserves the structure of individual particles tightly pressed against each other. Nevertheless, in the case of PP2%, in contrast to PP10%, there is a certain number of chains connecting the particles together. An example of combined PP2% grains is shown by the arrow in Figure 2d. The enlarged number of chains connecting grains confirms the greater ability to combine grains containing partially disentangled macromolecules. The grain size is similar in both materials and is typically 20–50 μm. The initial compaction process consolidated the powders into the solid samples of a shape suitable for ECMAE processing.

3.2. Crystallinity of materials

Conventionally sintered at elevated temperatures (close to or above the melting point), polymers exhibit two melting peaks, revealing the presence of both nascent and melt-recrystallized materials [50]. In addition, as melt-recrystallized polymers are less crystalline than nascent ones, partial melting is accompanied by a progressive loss of crystallinity degree [50]. That is why DSC tests were conducted to find out whether the crystallinity significantly changes during compaction and ECMAE sintering steps.

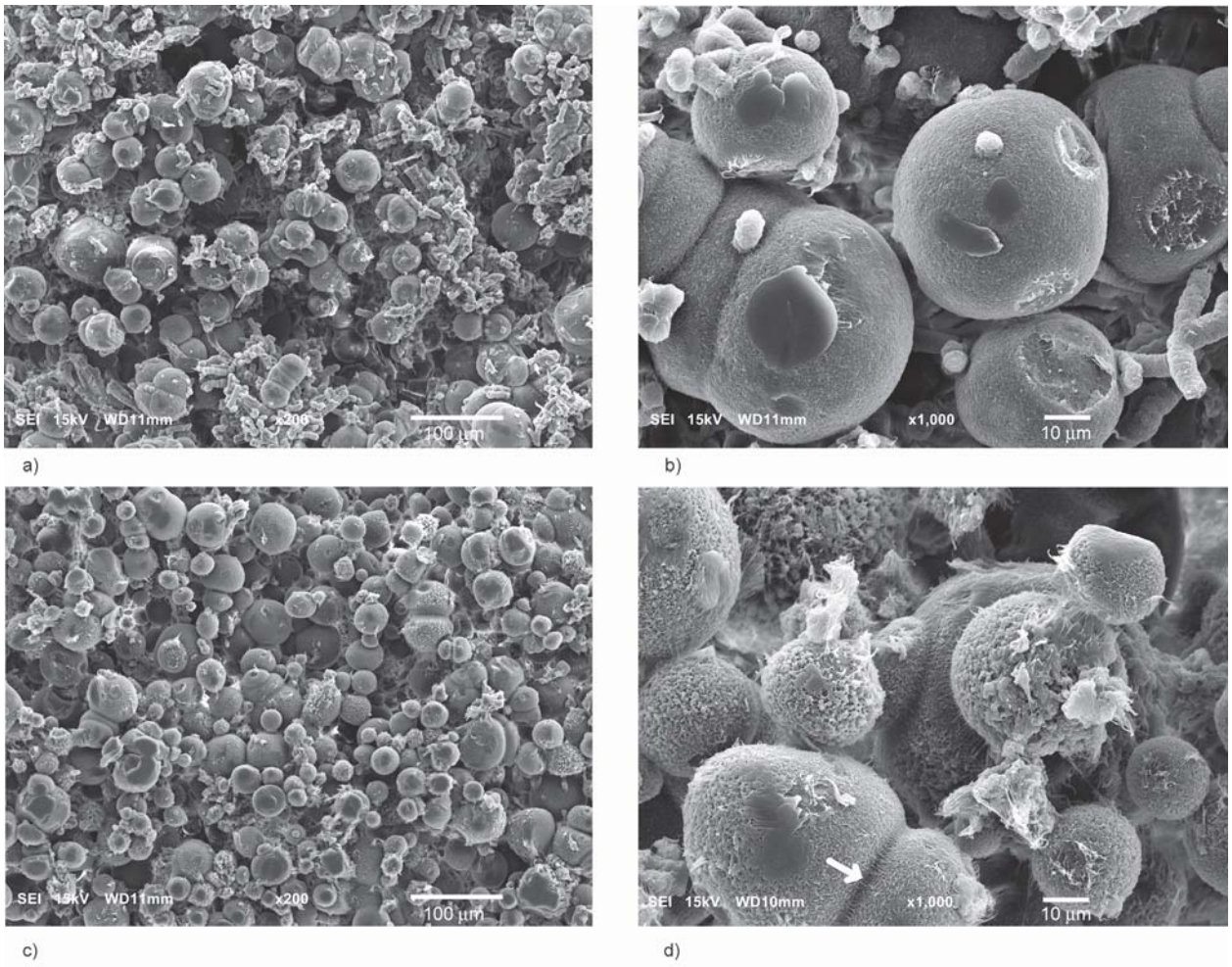

Figure 2. Morphologies of compacted polypropylene powders before ECMAE extrusion. Fractured samples were observed by SEM: (a–b) PP entangled (PP10%); (c–d) PP disentangled (PP2%).The arrow shows highly oriented fibrils, bonding two grains.

Figure 3 shows the DSC melting curves of nascent PP powders, preliminary compacted, as well as ECMAE-sintered PP. Table 1 provides detailed information on the melting temperature and crystallinity.

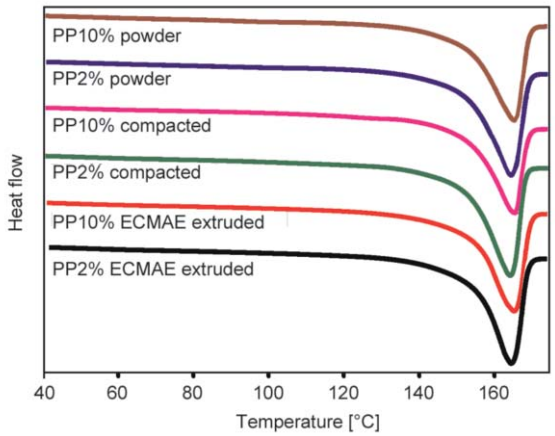

Figure 3. DSC melting curves of the PP nascent powders, after preliminary compacting and after ECMAE-sintering of PP. The curves are shifted vertically for better visualization.

It is seen that the thermograms of both ECMAE-sintered disentangled and entangled PP display a single melting peak centered at T_m of around 165 °C, originating from the nascent powder crystalline phase. Besides, the lack of any low-temperature peaks associated with the melt-recrystallized phase demonstrates the absence of a recrystallization process during ECMAE sintering. At the same time, for both PP powders, the ECMAE sintering induced almost the same crystallinity degree increment of 5–9% (the powder crystallinities were 44–46% and the extrudate crystallinities were 51–53%), indicating that the content of the new crystallites formed in the extrudates was subequal.

A possible reason for increasing the degree of crystallinity of the extrudates may be the strain-induced crystallization, in which an initially amorphous phase becomes ordered during deformation and undergoes a phase transformation into a crystalline one [51]. This assumption is also confirmed by the fact that

Table 1. Thermal properties of PP2% and PP10%. T_m – melting temperature, ΔH_m – enthalpy of melting, X – crystallinity.

Material		T_m [°C]	ΔH_m [J/g]	X [%]
PP entangled (PP10%)	nascent powder	163.5	96.3	46.0
	after preliminary compacting	165.2	97.5	46.7
	after ECMAE	165.2	105.6	50.5
PP disentangled (PP2%)	nascent powder	164.7	92.2	44.0
	after preliminary compacting	161.4	97.6	46.7
	after ECMAE	164.6	110.0	52.6

preliminary annealing at extrusion temperature for 15 minutes and subsequent compaction without straining did not lead to an important change in the degree of crystallinity (Table 1). Since the strain-induced crystallization could occur everywhere in the amorphous phase, it can be assumed that the new crystallites were able to form both at interfaces and within the particles.

Interestingly, in the literature can be found that the sintering by equal channel angular pressing with back pressure (ECAE-BP) leads to a decrease in the crystallinity degree of polymers [38, 39]. The reason for different behavior in changing the degree of crystallinity in the case of ECAE-BP and ECMAE can be a different value of the accumulated deformation (2.0 in the case of ECAE-BP and 8.5 for ECMAE). According to Deplancke *et al*. [26], the deformation required for the strain-induced crystallization is achieved with a high degree of drawing, $\lambda \approx 3$. Thus, strain-induced crystallization, which happens at high strain, could not provide the limitation of the chain interdiffusion at low strains, and finally, sufficient amounts of the chain could diffuse through the interfaces of the sintered PP products.

3.3. Interdiffusion process and accommodation of deformation

Although the crystalline phase can partially transform into the amorphous phase during plastic deformation and thus participate in the interdiffusion process, the observed increase in the degree of crystallinity in the case of ECMAE (Table 1) indicates a low probability of this process even at high strain region. Thus, at ECMAE, particles of PP would coalesce throughout the interdiffusion of chains of amorphous phase across their contact interfaces. Wherein the amorphous phase with a lower degree of entanglement should be more capable for diffusion across particles contact regions.

Indeed, in the framework of the reptation theory, which describes the diffusion of chain polymers in the rubbery state, the reptation time, τ, correlates with the time needed for the chain to pass over the interface [52–54] and can be calculated via Equation (2):

$$\tau = 3\tau_s \left(\frac{M}{M_e}\right)^3 \left[1 - \left(\frac{M_e}{M}\right)^{0.5}\right]^2 \tag{2}$$

where τ_s is given by Equation (3):

$$\tau_s = \frac{\rho \langle R \rangle^2 \frac{M_e^2}{M}}{3\pi^2 k_B T m_o} \tag{3}$$

where τ_s is the relaxation time in monomeric scale, M is the molecular mass, M_e is the molecular mass between entanglement knots, ρ is monomeric friction coefficient, $\langle R \rangle$ is the radius of gyration, k_B is Boltzmann constant, T – absolute temperature, m_o – the molecular mass of monomer [55]. Calculations based on known M_e values and data from Vega *et al*. [55] show that the reptation time is 3 s for the disentangled PP2% and 5 s for the entangled PP10%, *i.e*., the ratio of these times is equal to 0.6. Hence, at the same extrusion temperature, the disentangled PP has a shorter reptation time than entangled PP, which indicates the less restraining effect of neighboring chains on interdiffusion in the former case. However, since the presence of the crystalline phase limits the mobility of macromolecules, fragments of the macromolecules (so-called 'slacks' [56]) rather than entire chains participate in the consolidation process. The calculated reptation times are shorter than the duration of ECMAE experiments.

In solidified polymers, all entanglement knots are rejected from crystals into amorphous layers, accumulated there mostly without further disentanglement. Since the entanglement knots are formed by the crossings of two chains and the formation of an entanglement knot by the three chains is less probable, then the network of entanglements can be treated at first approximation as two dimensional, and then the number of entanglement knots is reciprocal to the second power of M_e. In PP2% the M_e is equal to 18 000 g/mol while in the virgin PP M_e is 9900 g/mol and in

PP10% is 12 600 g/mol [20] hence the number of knots in PP2% is 3.3 times less and in PP10% is 1.6 times less than in the virgin PP.

Earlier authors modeled consolidation using the classic reptation theory, but Deplancke and coworkers [25, 26] have demonstrated that diffusion and entanglement across grain boundaries can take place much more rapidly than is predicted by reptation-based models by following different kinetics. Working on UHMWPE moldings made from as-polymerized reactor powder, they carried out tensile tests at 200 °C, which showed that the effects of sintering time t_s on stress-strain curves were relatively small, with t_s ranging from 0.25 to 100 hours, while the sintering temperature had a much stronger effect on the mechanical properties. From these observations, Deplancke and coworkers [25, 26] concluded that chain diffusion and entanglement are dominated by 'sideways' motions (normal to the chain axis) of large chain loops, which are able to bond particles together much more rapidly than the chain-end reptation. In the present context, the speed at which chain loops bond particles together during compression molding raises questions about their ability to resist gradual pull-out during mechanical tests at room temperature. If the mechanism of the sideways motion of large chain loops is correct, the disentangled PP2% sample should sinter more than PP10% and entangled PP nascent powder. The deeper the chains diffuse and overlap, the larger is the interpenetration distance and the higher the interfacial volume, as the particles coalesce more.

The higher interfacial volume of disentangled PP compared to entangled PP is confirmed by SEM investigation. Micrographs shown in Figure 4 indicate that the particles coalesce more in the case of disentangled PP. Moreover, the particles in the disentangled PP sample completely coalesce with each other to the point that almost no intraparticle pores are observed in the micrographs. In contrast, more entangled PP10% shows both voids and cracks at the internal borders in the polymer (marked by red squares). These results are further confirmed by the compression test results.

In contrast to conventional sintering, which is preceded by a densification stage, in the case of ECMAE, polypropylene grains move, rotate, and also collapse and plastically deform, thus adjusting spatially to each other. The different deformation abilities of entangled/disentangled PP could exert a significant effect on the ability of a material to completely accommodate plastic deformation. Otherwise, accommodation is only partial. As a result, voids or micro discontinuities appear between grains, and there is no reduction of surface energy necessary for the effective ECMAE sintering.

Details of the structures were further revealed by observations of microtome sliced and etched samples. Figure 5 shows that for entangled PP after ECMAE-sintering, a spherulitic structure is observed with clear boundaries between spherulites. In contrast, in the case of disentangled PP, the spherulites are poorly visible. It was hard to distinguish the inter-spherulitic boundaries, and the structure locally seems to be more homogeneous but oriented.

The more effective sintering in the case of PP2% sample was confirmed by the measurements of extrudates densities using pycnometry. The obtained values were 0.8940 g/cm^3 for PP2% and 0.8723 g/cm^3 for PP10%. Assuming the density of amorphous PP

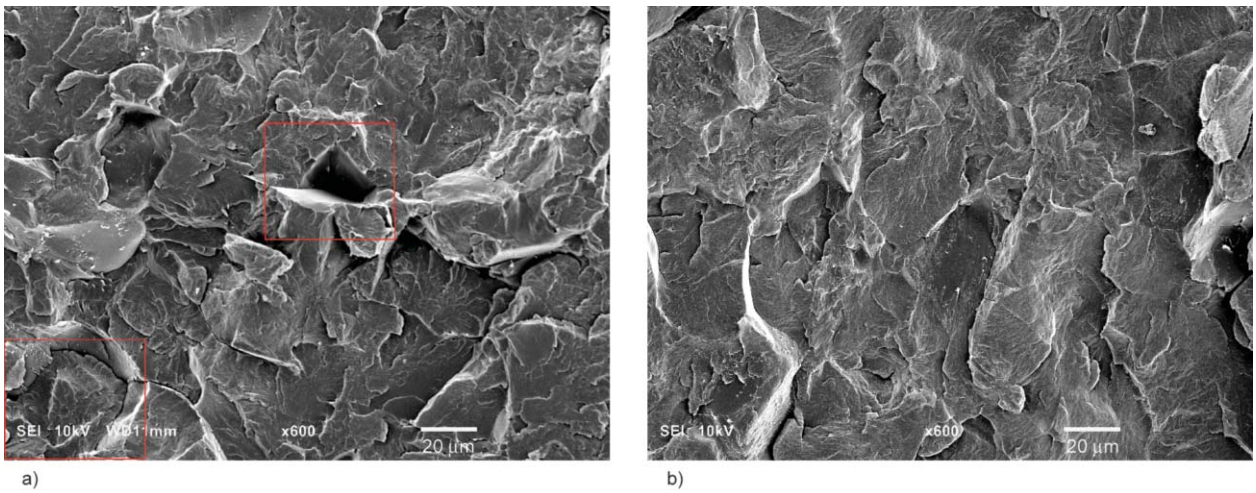

Figure 4. SEM images of cryo-fractured surfaces of entangled (a) and disentangled (b) PP sintered by ECMAE.

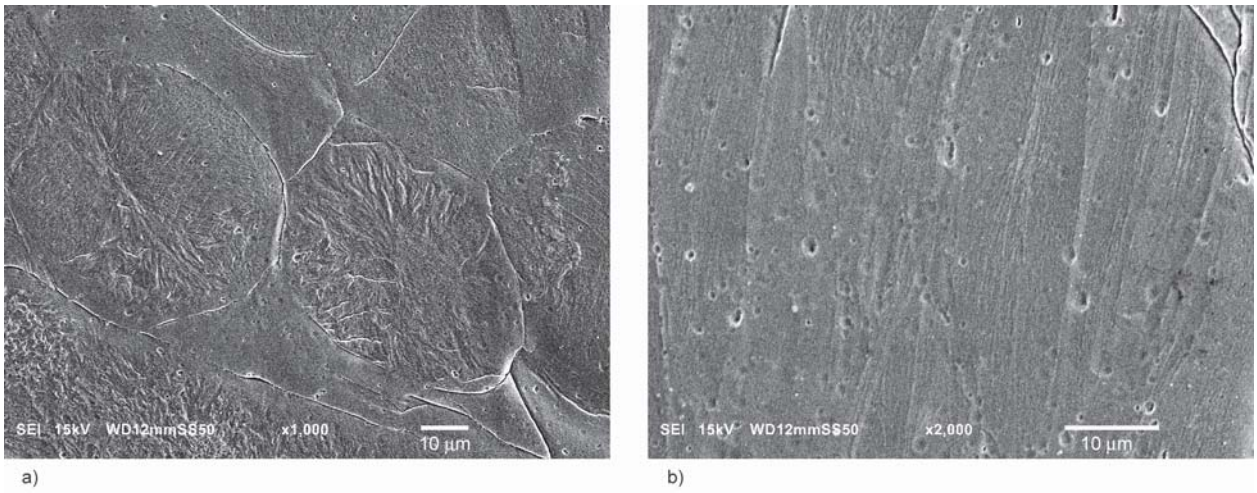

Figure 5. SEM images of entangled (a) and disentangled (b) PP sintered by ECMAE. Sample surfaces were prepared by ultra-microtoming and etched with permanganic etchant.

as $\rho_a = 0.855$ g/cm^3, the density of crystalline PP as $\rho_c = 0.946$ g/cm^3 and crystallinities of extrudates (X) as in Table 1, *i.e.*, 0.505 for PP10% and 0.526 for PP2%, it is possible to calculate the contribution of voids V_o, to the total volume, V, in each material using Equation (4):

$$\frac{V_o}{V} = 1 - \frac{\rho X}{\rho_c} - \frac{\rho(1-X)}{\rho_a} \tag{4}$$

The voids contribution was determined as 3.0% for PP10% and only 0.7% for PP2%, which confirms a more efficient packing for initially less entangled polymer (PP2%).

The transformation of the structure is also accompanied by rearrangements at the lamellar scale. It is known that exposure to high pressure can lead to phase transitions in PP [57]. The phase transitions in semicrystalline polymers were also observed in the case of solid-state ram extrusion [58] as well as in the ECMAE [59]. However, such a phase transition is not observed in the case of ECMAE-sintering of PP. Figure 6 shows the diffraction for the PP 10% sample after ECMAE extrusion, also very similar to the diffraction for PP2% sample (not shown). Peaks representing scattering from planes in monoclinic α crystals are visible while the γ-crystallographic form is not detected (the (117) refection of γ-form at around $2\theta \approx 20°$ is not seen while (130) reflection of α form is well recognized).

The orientation of the crystal phase was analyzed based on 2D WAXS data. Figure 7 shows the scattering patterns for both kinds of polypropylene samples investigated in two perpendicular directions. The scattering of the X-ray beam oriented in the direction

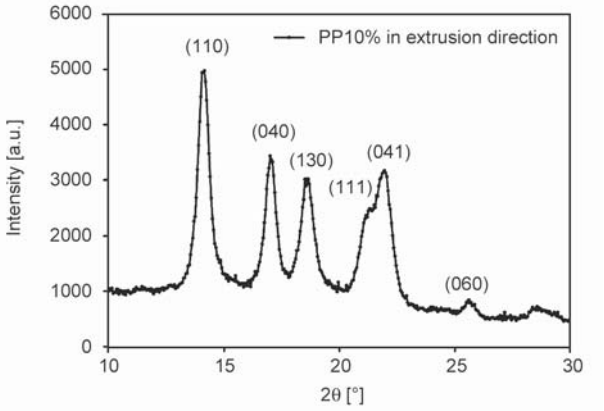

Figure 6. The WAXS diffractogram of PP10% sample after ECMAE extrusion. X-ray beam was directed in the extrusion direction.

of extrusion is shown in Figures 7a, 7c. Some relatively weak orientation of the material is visible, similar in both polymers: PP2% and PP10% and resulting from the alternating character of deformation in consecutive kinks of ECAE, which leads to nearly complete removal of the macroscopic molecular orientation after every second kink of ECAE [46]. However, significant differences in the diffraction images occur when the observation is carried out in the direction perpendicular to the extrusion (Figure 7b, 7d). The weak orientation is visible in the PP10% sample, while substantial orientation occurs in the PP2% sample. The vertical scattering coming from planes (110), (040), (130) of α-phase containing macromolecule chains (Figure 7d) shows that these chains are oriented with some tilt with respect to the extrusion direction. Crystalline texturing of the (hk0) planes with a tilted orientation of the chains with respect to the ECAE extrusion direction were also observed in

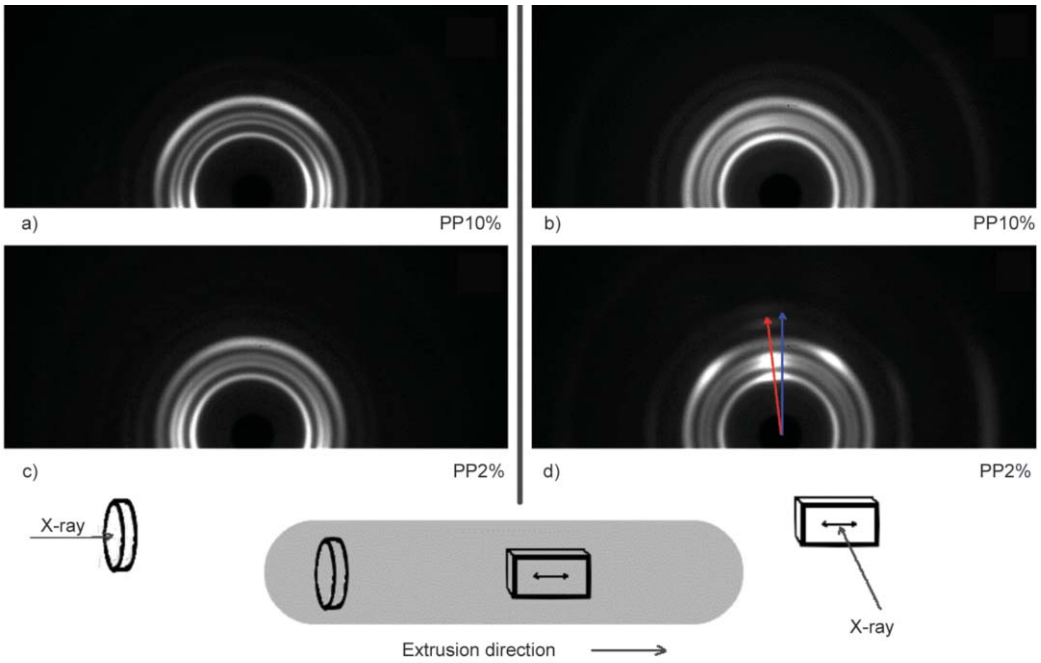

Figure 7. X-ray diffraction patterns for samples after ECMAE extrusion: a) PP 10% observed in the direction of extrusion, b) PP10% observed in the direction perpendicular to extrusion, c) PP2% observed in the direction of extrusion, d) PP2% observed in the direction perpendicular to extrusion.

the case of ECAE of bulk polypropylene samples [60–62]. The orientation of polymer chain fragments in simple shear can be described as flow in low Reynolds number hydrodynamics (ratio of inertia and viscous stress). It was well and thoroughly discussed in the monograph of Happel and Brenner [63] and also in the theory of dispersive mixing [64].

For samples oriented as in Figures 7b and 7d, diffractograms in vertical directions were made. From these diffractograms, the peak widths at half height were determined and the characteristic crystal sizes were calculated using the Scherrer's approach. The crystal size in the direction perpendicular to (hkl) planes, L_{hkl}, could be calculated from the half-width of the diffraction peak by using Equation (5):

$$L_{hkl} = \frac{0.9\lambda}{\beta \cos\theta} \tag{5}$$

where λ is the wavelength, β is the half-width of diffraction peak, and θ is the Bragg angle. Measurements were made for scattering on planes (110) and (040). In the case of PP10%, the same values were obtained for both planes, *i.e.*, $L_{110} = L_{040} = 12.7$ nm. Smaller crystal sizes were obtained for the PP2% sample: $L_{110} = 11.9$ nm and $L_{040} = 11.8$ nm. Since a decrease in the density of chain entanglements does not affect the size of the crystals, it can be concluded that the crystal size values in PP2% sample alter more significantly due to ECMAE shearing.

The samples after ECMAE sintering were also subjected to SAXS tests, recording scattering images in similar directions as described in Figure 7. The patterns obtained in the direction of extrusion (Figure 8a, 8d) show little orientation of crystals for PP10% and virtually no orientation for PP2%. When the beam direction was perpendicular to the extrusion direction, the scattering indicates the significant orientation in the samples (Figure 8b, 8e). Since the maximum scattering intensities in deformed samples are close to those measured for the initial polymer, it can be considered that the scattering on nanometer voids in the structure is negligible. Measurements at the edge of the sample, where a skin effect could occur, did not show any significant differences, although the orientation of the structure was slightly larger there, giving sharper central scattering (Figure 8c, 8f).

Assuming that the crystals have lamellar shape and are packed in stacks, it was possible to determine the long periods of structure, based on the maxima on horizontal and vertical profiles ($I \cdot s^2$, where I is the intensity, s – scattering vector, I is corrected applying the Lorentz correction). From the scattering images it can be seen that in the horizontal (extrusion) direction, a larger number of oriented structures contribute

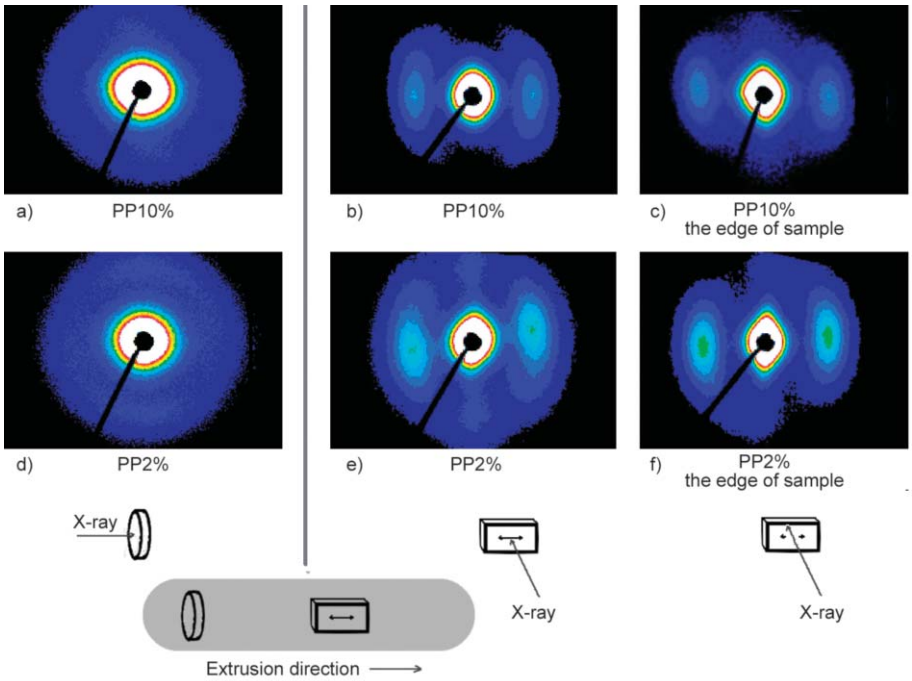

Figure 8. SAXS scattering from samples after ECMAE: a) PP10% observed in the direction of extrusion, b) PP10% observed in the direction perpendicular to extrusion, c) PP10% observed in the direction perpendicular to extrusion, but near the edge of sample, d) PP2% observed in the direction of extrusion, e) PP2% observed in the direction perpendicular to extrusion, f) PP2% observed in the direction perpendicular to extrusion, but near the edge of sample.

Table 2. Long periods of structures determined from the SAXS patterns. The numbers in parentheses relate to: the values of the long period, thickness of crystalline part and the thickness of amorphous part in the lamellar stacks, respectively, all determined from the correlation function.

X-ray direction	Scanning profile direction	Long period [nm]	
		PP10%	PP2%
In extrusion direction	Horizontal	12.3 (12.2/9.2/3.0)	12.8 (12.1/9.1/3.0)
	Vertical	14.9 (13.5/7.3/6.2)	13.9 (13.3/7.3/6.0)
Perpendicular to extrusion direction	Horizontal	15.9 (12.9/9.6/3.3)	16.3 (15.5/11.7./3.8)
	Vertical	15.1 (14.6/8.4/6.2)	14.3 (13.3/7.6/5.7)
Perpendicular to extrusion direction, measured on the edge	Horizontal	16.1 (15.7/11.7/4.0)	16.7 (15.2/11.2/4.0)
	Vertical	13.5 (13.0/6.8/6.2)	13.3 (12.3/6.3/6.0)

to a long period than in the vertical direction. The determined long periods of structures are summarized in Table 2. This table also includes long periods and divisions into the crystalline and amorphous parts, determined from the same SAXS data by the electron density correlation function method. The measured values of the long period were in the range of 12.3–16.7 nm. With a degree of crystallinity of 51–53%, it meant that the thickness of lamellar crystals was 6–8 nm. Measurements in the PP2% and PP10% skin area gave similar results as measurements in volume. The long period values were slightly larger in the direction of extrusion, which indicated greater crystal thickness than in the perpendicular (vertical) direction. Calculations with the use of the correlation function confirmed the above and additionally showed that the lamellae with a normal in the direction of deformation were thicker than lamellae with a normal perpendicular to this direction.

Figures 4 and 5 show that in the entangled PP10% polymer after the ECMAE process, visible cracks remain at the boundaries between the spherulites, and

voids are present in the structure in contrast to PP2%. It means that the tested materials should differ significantly in mechanical properties.

The samples for microhardness tests were cut in three directions: in a plane perpendicular to the extrusion direction and in two planes containing the extrusion direction but rotated by 45 degrees. The results are presented in Table 3. Comparing the microhardness of samples cut in the selected planes, it can be seen that the microhardness measured for PP2% is almost two times higher than those for PP10%. This confirms a much better consolidation of the PP2% material processed by ECMAE than PP10%. Measurements made in two selected planes containing the extrusion direction, but rotated by 45 degrees, showed significant differences in the microhardness values. The geometry of the ECMAE device is such that although the material obtains a uniform degree of deformation, its structure is oriented with a symmetry plane instead of axial symmetry.

Compression tests were performed to avoid premature fracture and cracking as it may occur in the tensile deformation. Figure 9 presents the stress-strain curves of compressed disentangled and entangled PP samples sintered by ECMAE. Evidently, the disentangled PP is characterized by a significantly higher yield strength as compared to the entangled PP (Table 4). However, they have similar Young moduli, which is probably the result of an equal crystallinity value.

The measured values of the modulus of elasticity are relatively small, weakly depending on the direction of compression, and are slightly higher for more entangled polypropylene. The modulus of elasticity is mainly dependent on the behavior of the amorphous phase confined between lamellar crystals. There is a scarcity of those data: the amorphous phase between lamellar crystals in polyethylene has a modulus of the order of 200 MPa [65, 66], but there are no such data for polypropylene. For further data analysis, we may assume a similar value of the modulus of polypropylene confined and entangled amorphous phase at room temperature. Disentangled confined amorphous layers of polypropylene must exhibit significantly lower modulus in compression

Table 3. Microhardness values [MPa] for PP2% and PP10%.

In the plane perpendicular to the extrusion direction		In the plane of the extrusion direction		In the plane at the angle of 45° to the plane of the extrusion direction	
PP2%	**PP10%**	**PP2%**	**PP10%**	**PP2%**	**PP10%**
57	28	65	34	35	19

Table 4. Mechanical properties of PP2% and PP10%.

		In the direction of extrusion		Perpendicular to the direction of extrusion	
		PP2%	**PP10%**	**PP2%**	**PP10%**
Elastic modulus	[MPa]	420	430	360	390
Yield stress	[MPa]	43.5	12.6	53.9	27.0
Compression ratio at yield		1.14	1.11	1.15	1.10

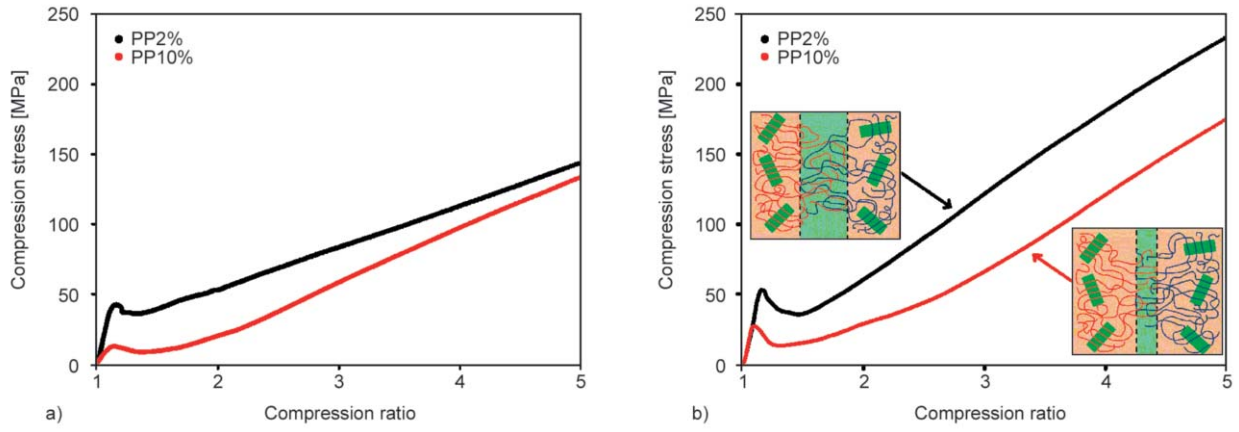

Figure 9. The stress-strain curves of compressed entangled and disentangled PP samples sintered by ECMAE. The samples were deformed in the direction along (a) and perpendicular (b) to the extrusion direction.

because crystalline species of partially disentangled PP are characterized by substantially lower modulus [20]. These observations agree with the observed moduli as depicted in Table 4. Considering the consolidation of the material by ECMAE sintering, the yield stress should be analyzed. According to the current knowledge, the yield stress is determined by the easiest crystallographic slip system. Since the crystals in PP2% are significantly oriented due to ECMAE the compressive stress must be sufficiently high in order to generate sufficient shear stress in the oriented slip planes. The easiest slip system for the alpha crystals of PP is (100)[001], requiring the generation of shear stress at the level of 22.6 MPa [67]. In a uniaxial compression test, such slip will require at least 45.2 MPa of uniaxial compression stress for the (100) crystallographic planes being oriented at the optimal angle of 45°. It can be seen from Table 4 that the yield stress of PP2% samples is in this range: 43.5 MPa in the extrusion direction and 53.9 MPa in the perpendicular direction. Evidently, the difference is caused by the strong orientation of crystals with macromolecular chains and (100) planes in the extrusion direction. Hence in order to reach the yield, higher compressive stress is required. On the other hand, PP10% shows much lower values of the stress at the yield point, which indicates that the plastic deformation resulted from a number of weak elements and defects due to much lower compactness and cohesion.

High load values that the PP2% sample could bear (*i.e.*, yield strength) mean also significantly enhanced interfacial strength [50]. Since the degree of crystallinity of ECMAE-sintered entangled and disentangled PP is approximately the same (Table 1), it can be concluded that the main contribution to the enhancement of interfacial strength is by chains located at the interphase. The observed almost two times higher values of yield strength in the case of PP2% as compared to PP10% (Table 4) are a qualitative sign of an improvement in the interfacial strength associated with chain penetration by reptation and chain loops sideways motion across the interfaces of powder particles. Thus, these processes determine an improvement in the interfacial strength during ECMAE powder sintering. The lower the entanglement degree in the nascent PP powders, the more PP chains are capable of crossing the interfaces in the process of ECMAE-sintering.

4. Conclusions

Samples of the same polypropylene, but significantly different in the density of entanglement of macromolecules, were subjected to the plastic deformation by extruding through the equal channel multi-angle device, i.e., using the ECMAE method. Already at the stage of preliminary consolidation of polymer powders, significant differences were noticed. Grains of disentangled polypropylene being compressed into a solid-state more easily compacted together. It was clearly visible in the microscope. The reason was the enhanced mobility of macromolecules in less entangled polymer by reptation or by the sideway motion of chain loops.

The main process of deformation was extrusion through the multichannel device. Even the external appearance after the ECMAE process shows the greater cohesiveness of grains in polypropylene, having initially limited entanglement density. This was confirmed by the observations with scanning electron microscopy, showing that voids in the structure between grains, spherulites, and cracks along the boundaries of spherulites were visible in processed PP10%. Such phenomena, potentially worsening the mechanical properties, were not visible in the case of PP2%, where the micro grains of PP2% powder bonded efficiently.

In addition to the efficiency of sintering, the subject of our interest was how the internal structure of polypropylene changes due to extrusion via the ECMAE method. Orientation of the material was expected. The SEM micrographs in Figure 5 show the elongated structure of spherulites in PP10% and the destroyed spherulitic structure in PP2%. X-ray examinations using the WAXS method evidenced the material orientation in the direction of extrusion, especially in the case of the PP2% sample. On the other hand, SAXS studies showed that lamellar stacks are preferentially oriented in the direction of extrusion. It was determined that the long periods of structure and the thickness of the lamellae are greater in the direction of extrusion than in the direction perpendicular to it. These differences are slightly larger in PP2%. DSC measurements showed that the orientation in the ECMAE process causes an increase in crystallinity due to the favorable orientation of the macromolecules.

The mechanical properties were affected by the orientation of crystallographic (100) planes with the

easiest (100)[001] crystallographic chain slips and greater structural integrity. During uniaxial compression, polypropylene, having initially lower entanglement density of macromolecules showed a slightly lower elastic modulus value, resulting from this reduced entanglement density in the amorphous layers between lamellar crystals. Very significant differences appeared at the yield point. PP2% exhibits the yielding that can be ascribed to the (100)[001] chain slips in alpha crystals. It also depends on the direction of deformation in relation to the direction of extrusion: even higher when compressed along extrusion direction. Activation of crystallographic slips during compression is direct evidence of high compactness and cohesion of less entangled PP2% after passing the ECMAE. On the contrary PP10% demonstrates two-three times lower values of stress at the yield point, indicating that yielding occurs through a series of weak elements and defects due to much poorer compactness and cohesion. Therefore, mechanical tests confirmed that the ECMAE process is much more effective for sintering PP with lower macromolecular entanglement density.

Acknowledgements

Statutory fund of the Centre of Molecular and Macromolecular Studies, Polish Academy of Sciences is acknowledged. The personal exchange was financed by the Polish Academy of Sciences and National Academy of Sciences of Ukraine under the agreement for the years 2018-2020.

References

[1] Eckstein A., Suhm J., Friedrich C., Maier R-D., Sassmannshausen J., Bochmann M., Mülhaupt R.: Determination of plateau moduli and entanglement molecular weights of isotactic, syndiotactic, and atactic polypropylenes synthesized with metallocene catalysts. Macromolecules, **31**, 1335–1340 (1998). https://doi.org/10.1021/ma971270d

[2] Litvinov V. M., Ries M. E., Baughman T. W., Henke A., Matloka P. P.: Chain entanglements in polyethylene melts. Why is it studied again? Macromolecules, **46**, 541–547 (2013). https://doi.org/10.1021/ma302394j

[3] Fetters L. J., Lohse D. J., Colby R. H.: Chain dimensions and entanglement spacings. in 'Physical properties of polymers handbook' (ed.: Mark J. E.), Springer, New York, 447–454 (2007). https://doi.org/10.1007/978-0-387-69002-5_25

[4] Robelin-Souffache E., Rault J.: Origin of the long period and crystallinity in quenched semicrystalline polymers. Macromolecules, **22**, 3581–3594 (1989). https://doi.org/10.1021/ma00199a015

[5] Tervoort-Engelen Y., Lemstra P. J.: Morphology of nascent ultra-high molecular weight polyethylene reactor powder – Chain extended versus chain folded crystals. Polymer Communications, **32**, 343–345 (1991).

[6] Sano A., Iwanami Y., Matsuura K., Yokoyama S., Kanamoto T.: Ultradrawing of ultrahigh molecular weight polyethylene reactor powders prepared by highly active catalyst system. Polymer, **42**, 5859–5864 (2001). https://doi.org/10.1016/S0032-3861(00)00899-5

[7] Okuyama H., Kanamoto T., Porter R. S.: Solid-state deformation of polytetrafluoroethylene powder. Journal of Materials Science, **29**, 6485–6494 (1994). https://doi.org/10.1007/BF00354009

[8] Huang Y-F., Xu J-Z., Zhang Z-C., Xu L., Li L-B., Li J-F., Li Z-M.: Melt processing and structural manipulation of highly linear disentangled ultrahigh molecular weight polyethylene. Chemical Engineering Journal, **315**, 132–141 (2017). https://doi.org/10.1016/j.cej.2016.12.133

[9] Pandey A., Champouret Y., Rastogi S.: Heterogeneity in the distribution of entanglement density during polymerization in disentangled ultrahigh molecular weight polyethylene. Macromolecules, **44**, 4952–4960 (2011). https://doi.org/10.1021/ma2003689

[10] Zwijnenburg A., Pennings A. J.: Longitudinal growth of polymer crystals from flowing solutions III. Polyethylene crystals in Couette flow. Colloid and Polymer Science, **254**, 868–881 (1976). https://doi.org/10.1007/BF01775411

[11] Smith P., Lemstra P. J.: Ultrahigh-strength polyethylene filaments by solution spinning/drawing, 2. Influence of solvent on the drawability. Die Makromolekulare Chemie, **180**, 2983–2986 (1979). https://doi.org/10.1002/macp.1979.021801220

[12] Smith P., Lemstra P. J.: Ultra-drawing of high molecular weight polyethylene cast from solution. Colloid and Polymer Science, **258**, 891–894 (1980). https://doi.org/10.1007/BF01566246

[13] Bu H., Gu F., Bao L., Chen M.: Influence of entanglements on crystallization of macromolecules. Macromolecules, **31**, 7108–7110 (1998). https://doi.org/10.1021/ma980713q

[14] Liu C. Y., Morawetz H.: Kinetics of the unfolding of collapsed polystyrene chains above the glass transition temperature. Macromolecules, **21**, 515–518 (1988). https://doi.org/10.1021/ma00180a039

[15] Wang X., Liu R., Wu M., Wang Z., Huang Y.: Effect of chain disentanglement on melt crystallization behavior of isotactic polypropylene. Polymer, **50**, 5824–5827 (2009). https://doi.org/10.1016/j.polymer.2009.10.002

[16] Lemstra P. J., van Aerle N. A., Bastiaansen C. W. M.: Chain-extended polyethylene. Polymer Journal, **19**, 85–98 (1987). https://doi.org/10.1295/polymj.19.85

[17] Pennings A. J., Smook J.: Mechanical properties of ultra-high molecular weight polyethylene fibres in relation to structural changes and chain scissioning upon spinning and hot-drawing. Journal of Materials Science, **19**, 3443–3450 (1984). https://doi.org/10.1007/BF00549837

[18] Yeh J-T., Chang S-S., Wu T-W.: Effect of the ultradrawing behavior of gel films of ultrahigh-molecular-weight polyethylene and low-molecular-weight polyethylene blends on their physical properties. Journal of Applied Polymer Sciences, **107**, 854–862 (2008). https://doi.org/10.1002/app.26273

[19] Bartczak Z., Kozanecki M.: Influence of molecular parameters on high-strain deformation of polyethylene in the plane-strain compression. Part I. Stress-strain behavior. Polymer, **46**, 8210–8221 (2005). https://doi.org/10.1016/j.polymer.2005.06.100

[20] Krajenta J., Pawlak A., Galeski A.: Deformation of disentangled polypropylene crystalline grains into nanofibers. Journal of Polymer Science Part B: Polymer Physics, **54**, 1983–1994 (2016). https://doi.org/10.1002/polb.24105

[21] Ogita T., Kawahara Y., Soga Y., Matsuo M.: Morphology and mechanical properties of ultrahigh molecular weight polypropylene prepared by gelation/crystallization at various temperatures. Colloid and Polymer Science, **270**, 833–839 (1992). https://doi.org/10.1007/BF00657727

[22] Ikeda Y., Ohta T.: The influence of chain entanglement density on ultra-drawing behavior of ultra-high-molecular-weight polypropylene in the gel-casting method. Polymer, **49**, 621–627 (2008). https://doi.org/10.1016/j.polymer.2007.11.043

[23] Chen J., Si X., Hu S., Wang Y., Wang Y.: The preparation and study on ultrahigh molecular weight polypropylene gel-spun fibers. Journal of Macromolecular Science Part B: Physics, **47**, 192–200 (2008). https://doi.org/10.1080/00222340701748677

[24] Pawlak A., Krajenta J., Galeski A.: Cavitation phenomenon and mechanical properties of partially disentangled polypropylene. Polymer, **151**, 15–26 (2018). https://doi.org/10.1016/j.polymer.2018.07.033

[25] Deplancke T., Lame O., Rousset F., Aguili I., Seguela R., Vigier G.: Diffusion versus cocrystallization of very long polymer chains at interfaces: Experimental study of sintering of UHMWPE nascent powder. Macromolecules, **47**, 197–207 (2014). https://doi.org/10.1021/ma402012f

[26] Deplancke T., Lame O., Rousset F., Seguela R., Vigier G.: Mechanisms of chain reentanglement during the sintering of UHMWPE nascent powder: Effect of molecular weight. Macromolecules, **48**, 5328–5338 (2015). https://doi.org/10.1021/acs.macromol.5b00618

[27] Doi M., Edwards S. F.: The theory of polymer dynamics. Oxford University Press, Oxford (1986).

[28] Kim Y. H., Wool R. P.: A theory of healing at a polymer-polymer interface. Macromolecules, **16**, 1115–1120 (1983). https://doi.org/10.1021/ma00241a013

[29] Bousmina M., Qiu H., Grmela M., Klemberg-Sapieha J. E.: Diffusion at polymer/polymer interfaces probed by rheological tools. Macromolecules, **31**, 8273–8280 (1998). https://doi.org/10.1021/ma980562r

[30] Rastogi S., Kurelec L., Lemstra P. J.: Chain mobility in polymer systems: On the borderline between solid and melt. 2. Crystal size influence in phase transition and sintering of ultrahigh molecular weight polyethylene *via* the mobile hexagonal phase. Macromolecules, **31**, 5022–5031 (1998). https://doi.org/10.1021/ma980261h

[31] Rastogi S., Kurelec L., Lippits D., Cuijpers J., Wimmer M., Lemstra P. J.: Novel route to fatigue-resistant fully sintered ultrahigh molecular weight polyethylene for knee prosthesis. Biomacromolecules, **6**, 942–947 (2005). https://doi.org/10.1021/bm0493638

[32] Gao P., Cheung M. K., Leung T. Y.: Effects of compaction pressure on cohesive strength and chain mobility of low-temperature compacted nascent UHMWPE. Polymer, **37**, 3265–3272 (1996). https://doi.org/10.1016/0032-3861(96)88472-2

[33] Segal V. M.: Materials processing by simple shear. Materials Science and Engineering: A, **197**, 157–164 (1995). https://doi.org/10.1016/0921-5093(95)09705-8

[34] Nakashima K., Horita Z., Nemoto M., Langdon T. G.: Development of a multi-pass facility for equal-channel angular pressing to high total strains. Materials Science and Engineering: A, **281**, 82–87 (2000). https://doi.org/10.1016/S0921-5093(99)00744-3

[35] Zhang X., Gao D., Wu X., Xia K.: Bulk plastic materials obtained from processing raw powders of renewable natural polymers *via* back pressure equal channel angular consolidation (BP-ECAC). European Polymer Journal, **44**, 780–792 (2008). https://doi.org/10.1016/j.eurpolymj.2007.12.011

[36] He S., Bai H., Bai D., Ju Y., Zhang Q., Fu Q.: A promising strategy for fabricating high-performance stereocomplex-type polylactide products *via* carbon nanotubes-assisted low-temperature sintering. Polymer, **162**, 50–57 (2019). https://doi.org/10.1016/j.polymer.2018.12.032

[37] Xia K., Wu X., Honma T., Ringer S. P.: Ultrafine pure aluminium through back pressure equal channel angular consolidation (BP-ECAC) of particles. Journal of Materials Science, **42**, 1551–1560 (2007). https://doi.org/10.1007/s10853-006-0819-8

[38] Reinitz S. D., Engler A. J., Carlson E. M., van Citters D. W.: Equal channel angular extrusion of ultra-high molecular weight polyethylene. Materials Science and Engineering: C, **67**, 623–628 (2016). https://doi.org/10.1016/j.msec.21016.05.085

[39] Al-Goussous S., Wu X., Yuan Q., Xia K.: Back pressure equal channel angular consolidation of nylon 12. Materials Forum, **31**, 36–39 (2007).
[40] Zhang X., Wu X., Gao D., Xia K.: Bulk cellulose plastic materials from processing cellulose powder using back pressure-equal channel angular pressing. Carbohydrate Polymers, **87**, 2470–2476 (2012). https://doi.org/10.1016/j.carbpol.2011.11.019
[41] Bai Y., Zhang X., Xia K.: High strength biocomposites consolidated from hardwood particles by severe plastic deformation. Cellulose, **26**, 1067–1084 (2019). https://doi.org/10.1007/s10570-018-2125-4
[42] Bai Y., Zhang X., Xia K.: Biocomposites produced from hardwood particles by equal channel angular pressing without additives. Journal of Composite Science, **3**, 36/1–36/10 (2019). https://doi.org/10.3390/jcs3020036
[43] Beloshenko V. A., Varyukhin V. N., Voznyak A. V., Voznyak Y. V.: Equal-channel multiangular extrusion of semicrystalline polymers. Polymer Engineering and Science, **50**, 1000–1006 (2010). https://doi.org/10.1002/pen.21613
[44] Gennes P-G.: Scaling concepts in polymer physics. Cornell University Press, Ithaca (1979).
[45] Krajenta J., Safandowska M., Pawlak A.: The re-entangling of macromolecules in polypropylene. Polymer, **175**, 215–226 (2019). https://doi.org/10.1016/j.polymer.2019.05.015
[46] Beloshenko V. A., Voznyak A. V., Voznyak Y. V.: Control of the mechanical and thermal properties of semicrystalline polymers *via* a new processing route of the equal channel multiple angular extrusion. Polymer Engineering and Science, **54**, 531–539 (2014). https://doi.org/10.1002/pen.23583
[47] Krigbaum W. R., Uematsu I.: Heat and entropy of fusion of isotactic polypropylene. Journal of Polymer Science Part A: General Papers, **3**, 767–776 (1965). https://doi.org/10.1002/pol.1965.100030231
[48] Olley R. H., Hodge A. M., Bassett D. C.: A permanganic etchant for polyolefines. Journal of Polymer Science: Polymer Physics Edition, **17**, 627–643 (1979). https://doi.org/10.1002/pol.1979.180170406
[49] Galeski A., Bartczak Z., Kazmierczak T., Slouf M.: Morphology of undeformed and deformed polyethylene lamellar crystals. Polymer, **51**, 5780–5787 (2010). https://doi.org/10.1016/j.polymer.2010.10.004
[50] Salari M., Pircheraghi G.: Interdiffusion versus crystallization at semicrystalline interfaces of sintered porous materials. Polymer, **156**, 54–65 (2018). https://doi.org/10.1016/j.polymer.2018.09.054
[51] Larrañaga A., Lizundia E.: Strain-induced crystallization. in 'Crystallization in multiphase polymer systems' (eds.: Thomas S., M. Arif P., Gowdm E. B., Kalarikkal N.), Elsevier, Amsterdam, 471–508 (2018). https://doi.org/10.1016/B978-0-12-809453-2.00015-3
[52] Doi M., Edwards S. F.: Dynamics of concentrated polymer systems. Part 1. – Brownian motion in the equilibrium state. Journal of the Chemical Society, Faraday Transactions 2: Molecular and Chemical Physics, **74**, 1789–1801 (1978). https://doi.org/10.1039/f29787401789
[53] Graessley W. W.: Entangled linear, branched and network polymer systems – Molecular theories. Advances in Polymer Science, **47**, 67–117 (1982). https://doi.org/10.1007/BFb0038532
[54] Zulli F., Giordano M., Andreozzi L.: Onset of entanglement and reptation in melts of linear homopolymers: Consistent rheological simulations of experiments from oligomers to high polymers. Rheologica Acta, **54**, 185–205 (2015). https://doi.org/10.1007/s00397-014-0827-6
[55] Vega J. F., Rastogi S., Peters G. W. M., Meijer H. E. H.: Rheology and reptation of linear polymers. Ultrahigh molecular weight chain dynamics in the melt. Journal of Rheology, **48**, 663-678 (2004). https://doi.org/10.1122/1.1718367
[56] Hoffman J. D., Miller R.: Test of the reptation concept: Crystal growth rate as a function of molecular weight in polyethylene crystallized from the melt. Macromolecules, **21**, 3038–3051 (1988). https://doi.org/10.1021/ma00188a024
[57] Lezak E., Bartczak Z., Galeski A.: Plastic deformation of the γ phase in isotactic polypropylene in plane-strain compression. Macromolecules, **39**, 4811–4819 (2006). https://doi.org/10.1021/ma0605907
[58] Yin H-M., Xu H., Zhang J., Chen J-B., Lei J., Xu J-Z., Li Z-M.: Effects of extrusion draw ratio on the morphology, structure and mechanical properties of poly(L-lactic acid) fabricated using solid state ram extrusion. RSC Advances, **5**, 69016– 69023 (2015). https://doi.org/10.1039/C5RA10579J
[59] Beloshenko V. A., Voznyak A. V., Voznyak Y. V., Glasunova V. A., Konstantinova T. E.: Polyamide-6 structure modification by combined solid-phase extrusion. Polymer Engineering and Science, **52**, 1815–1820 (2012). https://doi.org/10.1002/pen.23123
[60] Phillips A., Zhu P-W., Edward G.: Simple shear deformation of polypropylene *via* the equal channel angular extrusion process. Macromolecules, **39**, 5796–5803 (2006). https://doi.org/10.1021/ma0607618
[61] Boulahia R., Gloaguen J. M., Zaïri F., Naït-Abdelaziz M., Seguela R., Boukharouba T., Lefebvre J. M.: Deformation behaviour and mechanical properties of polypropylene processed by equal channel angular extrusion: Effects of back-pressure and extrusion velocity. Polymer, **50**, 5508–5517 (2009). https://doi.org/10.1016/j.polymer.2009.09.050

[62] Wang T., Tang S., Chen J.: Effects of processing route on morphology and mechanical behavior of polypropylene in equal channel angular extrusion. Journal of Applied Polymer Science, **122**, 2146–2158 (2011). https://doi.org/10.1002/app.34335

[63] Happel J., Brenner H.: Low Reynolds number hydrodynamics. Prentice-Hall, Englewood Cliffs (1965). https://doi.org/10.1007/978-94-009-8352-6

[64] Meijer H. E. H., Janssen J. M. H., Anderson P. D.: Mixing of immiscible liquids. in 'Mixing and compounding of polymers' (ed.: Manas-Zloczower I.) Hanser, Munich, 41–182 (2009).

[65] Xiong B., Lame O., Chenal J-M., Rochas C., Seguela R., Vigier G.: Amorphous phase modulus and micro–macro scale relationship in polyethylene *via in situ* SAXS and WAXS. Macromolecules, **48**, 2149–2160 (2015). https://doi.org/10.1021/acs.macromol.5b00181

[66] Galeski A.: Strength and toughness of crystalline polymer systems. Progress in Polymer Science, **28**, 1643–1699 (2003). https://doi.org/10.1016/j.progpolymsci.2003.09.003

[67] Bartczak Z., Galeski A.: Yield and plastic resistance of α-crystals of isotactic polypropylene. Polymer, **40**, 3677–3684 (1999). https://doi.org/10.1016/S0032-3861(98)00614-4